

Investigation of Nitromethane Combustion Using Laser Induced Fluorescence

Said Ali El-busaidy

Supervisor: Elna H. Nilsson

Co-supervisor: Christian Brackmann

Master Thesis

May 2016



LUNDS
UNIVERSITET

Department of Physics
Division of Combustion Physics

Abstract

Pre-mixed nitromethane/air/nitrogen flames on a heat-flux burner are investigated at atmospheric pressure with equivalence ratios of $\Phi=0.8$ and $\Phi=1.2$. Flame thermometry and chemiluminescence spectrum were used to characterise the flame before carrying out saturated laser induced fluorescence on NO molecules. The temperature profile revealed three zones of nitromethane combustion with maximum temperature of 1400K for the lean and 1350K for the rich flame. The chemiluminescence spectrum showed that numerous radicals were produced and NO_2 was responsible for the flame yellow appearance especially in the lean case. The NO concentration profiles showed good agreement with global chemical equation calculations and previous studies despite some differences. The results indicated that nitrogen and NO are the main nitrogenous products of nitromethane combustion. The results will be used to validate chemical kinetic models of nitromethane combustion.

Acknowledgement

I would like to sincerely thank Christian Brackmann for allowing me the opportunity to do this thesis project. His help and explanations have made this an enjoyable experience. I have learned a lot from him. Secondly, I would like to thank Jenny Naucier and Elna H.Nilsson for their help and guidance in the chemistry involved during the thesis. I would like to express my gratitude to all the staff at the division combustion physics for your kindness and warmth during this period. Most of all I would like to thank my family and friends for their love , support and encouragement during my education. Finally, I would like to thank Swedish Institute scholarship for presenting me with the opportunity to do my masters education at Lund University.

Contents

1	Introduction	1
1.1	Motivation for combustion studies	1
1.2	Thesis Objective	2
2	Theory	3
2.1	Equivalence ratio	3
2.2	Nitromethane	3
2.3	Laser Induced Fluorescence	5
2.3.1	Fluorescence signal	6
3	Experimental method	9
3.1	Introduction	9
3.2	Burner setup	9
3.3	Temperature and flame chemiluminescence measurements	11
3.4	Laser Induced Fluorescence	12
3.5	NO concentration evaluation	14
4	Results and Discussion	17
4.1	Temperature measurements	17
4.2	Chemiluminescence spectra	20
4.3	LIF measurements	22
4.3.1	Excitation scan	22
4.3.2	2-D fluorescence images	24
4.3.3	NO concentration profiles	25
5	Outlook	29

Chapter 1

Introduction

1.1 Motivation for combustion studies

Fossil fuels are a major source of energy in the world. Despite the availability of ‘clean’ energy sources and numerous environmental and health hazards of combustion, fossil fuels, are estimated to account for 76 percent of the total energy production by 2020. This is according to a survey published by the world energy council in 2013 [1]. Recent advancement and use of technology in all aspect of human life, coupled with the annual increase in population has led to an increase in energy demand [1]. Therefore, it is important to study combustion to make the processes energy efficient and with lower pollution formation.

The combustion of fuels into their final products of water and carbon dioxide is complex and not completely understood as it involves many intermediate chemical reactions, for example the complete combustion of methane involves 149 reactions [2]. Since fossil fuels are non-renewable and resources are expected to eventually be depleted, a lot of research is currently being done in a bid to optimize the efficiency of this process resulting in less fuel consumption. Furthermore, some of the byproducts during combustion have serious health effects and cause environmental pollution. For example, combustion of hydrocarbons produces toxic oxides of sulphur and nitrogen. Renewable fuels from biomass have been introduced to supplement and reduce the dependency on fossil fuels. However, these fuels may include nitrogen, sulphur and alkali atoms in the fuel itself making pollutant formation more complex. Knowledge of the elementary reactions can be used to minimise these toxic oxides from being formed making the process environmentally friendly [3].

Laser spectroscopic techniques are commonly used for combustion diagnostics [3, 4]. This is achieved by probing atoms/molecules/particles in the flame with laser beams. The laser interaction with the flame atoms/molecules/particles produces light signals that are detected and provide information about the combustion. Measurements on species concentrations, temperature, particle properties and the flows of the flame can be achieved

using lasers. The technique used depends on the type of measurement to be carried out. For example, Laser induced fluorescence (LIF) is suitable for species concentration measurements, coherent anti-Stokes Raman spectroscopy (CARS) is suitable for temperature measurements while laser induced incandescence (LII) is suitable for soot volume fraction measurements [4].

Laser diagnostics have several advantages over physical probing of a flame. The measurements made are non-intrusive and therefore do not disrupt the flow and chemical reactions taking place. Laser techniques also enable studies of turbulent flames or highly explosive flames where measurements would normally be impossible to perform using other physical methods. The measurements have very good spatial and temporal resolution since a focused beam on the order of 10 micrometers can be achieved and lasers providing pulses with duration of 10 nanoseconds or shorter are available.

Since nitromethane is one of the simplest fuels containing nitro group, it is used as the prototype for reactions containing more complex energetic material [5]. Knowledge about its reactions can facilitate understanding of more complex fuels containing the nitro group. However, nitromethane combustion diagnostics so far has involved determination of laminar burning velocity[6] and kinetic modelling at different equivalence ratios [7] and pressure [5] [8]. Hence the present study was undertaken to further enhance the understanding of nitromethane combustion at atmospheric pressure. The results could be used to verify the accuracy of the predictions of the kinetic models.

1.2 Thesis Objective

The objective of the thesis is to increase the understanding of nitromethane combustion. This is accomplished by initially establish well defined flames suitable for laser diagnostics and modelling at two different equivalence ratios. This is accomplished by obtaining flat, stable, premixed flames, which are considered to be one dimensional. The combustion of nitromethane is then characterized by taking the temperature and spectral profile at two different equivalence ratios. Finally, the NO concentration during nitromethane combustion is measured using laser induced fluorescence (LIF).

The thesis is a part of on-going investigations of nitromethane combustion to be carried out. The results of this thesis and the additional experiments will be compared with detailed chemical kinetic modelling results and are also intended for publication.

Chapter 2

Theory

2.1 Equivalence ratio

The equivalence ratio Φ , is used to express the ratio of the fuel and oxidant concentration in a reactant mixture.

$$\phi = \frac{\text{(fuel-oxygen ratio)in real mixture}}{\text{(fuel moles-oxygen moles)in stoichiometric mixture}} \quad (2.1)$$

When the equivalence ratio is less than 1, the flame is said to be a lean flame. This means that the concentration of the oxidizer is higher than the concentration of the fuel in the mixture. Whereas when the equivalence ratio is more than 1, the flame is said to be a rich flame, in that the concentration of the fuel is higher than the concentration of the oxidizer in the mixture. When the equivalence ratio is 1, the flame is said to be stoichiometric. A stoichiometric flame is the ideal flame in that all the fuel and oxidizer molecules in the mixture are completely consumed forming carbon dioxide and water as the final products.

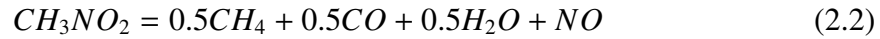
2.2 Nitromethane

Nitromethane is a highly flammable colorless liquid with chemical formula CH_3NO_2 . It has molecular weight of 61.04 g/mole and a density of 1.137 g/cm³ at 200 C [5]. It's freezing and boiling points at atmospheric pressure are 244.6 K and 374.35 K respectively [5]. It is a highly polar solvent with numerous industrial applications such as manufacturing of pesticides, pharmaceuticals and a cleaning solvent.

As a fuel, nitromethane can burn without oxidizer due to the presence of oxygen within its chemical structure. It is capable of delivering more power compared to other fuels like gasoline for the same quantity of fuel and practically, it is used as a racing car fuel.

Moreover, its high performance and reduced toxicity makes it an attractive alternative to hydrazine as a rocket fuel [5].

Earlier scientific work had concluded that nitrogen was the stable product of both the thermal decomposition and oxidation of nitromethane [9, 10, 11]. But the model of Guirguis et al. [12], instead predicted that NO was the stable product of thermal decomposition.

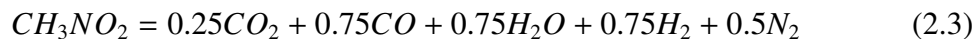


However, Boyer and Kuo's model showed that the NO formed will be reduced and consumed. Their prediction was validated with experimental data at high pressure between 3-15 MPa [5]. Furthermore, the model revealed three different zones for the consumption of nitromethane.

In the first zone, nitromethane was decomposed by breaking the C-N bond into CH₃ and NO₂ [5]. CH₃ being a highly reactive radical, is converted to CH₄ and CH₃O. CH₄ is relatively stable in this zone but CH₃O is converted to CO through a sequence of oxidation processes CH₃O-CH₂O-HCO-CO [8]. NO₂ is unstable at the temperatures in this zone, and is therefore converted to the more stable NO. However, a small amount of NO is converted to HNO and N₂O [5]. Therefore, at the end of zone 1, CH₂O, N₂O, HNO, CH₄ and NO are intermediate species of nitromethane combustion. While the concentrations of these intermediate species are low, CH₄ and NO are most abundant and reach their peak concentration in this zone.

In the second zone, all the intermediate species are completely consumed apart from CH₄ and NO. Some CH₄ and all CH₂O are consumed to produce CO, however, some CO is further oxidized to CO₂ [5]. HNO is converted to NO while N₂O is reduced by CO or H to N₂ [5]. These reactions cause the temperature of the reaction zone to increase.

In the third zone, all of the remaining NO and CH₄ is completely consumed to produce N₂, H₂, CO, CO₂ and H₂O as the final products [5]. This is where the flame achieves its maximum temperature. The total process can be described by a chemical equation according to equation 2.3



However, experimental work by De Jaegere and Van Tiggelen on a nitromethane+oxygen flame at low pressure, produced NO as the stable product according to the chemical equation 2.4, stating that the NO formed is not a reactive species [13]. Tian et al.[7] and Zhang et al. [8] models of nitromethane oxidation at low pressure agreed with this conclusion.



The chemical equation 2.4 is used to define the equivalence ratio of nitromethane combustion [6]. Despite having different stoichiometric equations for thermal decomposition and oxidation, and different NO_x final product, the combustion of nitromethane has 3 different reaction zones in both cases.

NO is a key species in the combustion of nitromethane and was therefore selected in this project for laser measurement for several reasons. It is produced in one of the most exothermic reactions in the combustion of nitromethane, that is, NO₂+H=NO, [14]. It is present in all the three reaction zones and participates in many other intermediate chemical reactions. Furthermore, its abundance in the flame gives a strong fluorescence signal favourable for detection.

2.3 Laser Induced Fluorescence

In laser induced fluorescence absorption of laser photons transfers molecules in the ground state to an excited state. When these molecules spontaneously decay back to the ground state, they release some radiation referred to as fluorescence [4]. The fluorescence radiation usually has longer wavelength compared with the original laser radiation. This is due to vibrational and rotational energy transfer by the molecules when in the excited state.

LIF is a very popular technique for combustion diagnostics due to its high sensitivity. It is capable of detecting species concentrations at ppm and even sub ppm level [4]. Many of the radicals investigated in combustion measurements are usually in concentrations below 100 ppm, and therefore LIF measurements are very suitable [4]. The LIF method also has the capability of doing 2-dimensional measurements by expanding the laser beam into a laser sheet and imaging the fluorescence distribution in the sheet.

The fluorescence radiation is due to the spontaneous emission. This is when the excited molecules, decay back to the ground state after a period of time (typically a few nanoseconds in an atmospheric pressure flame). The interactions are summarized in the 2-level model of the LIF process illustrated in the diagram in Figure 2.1 and analysed in detail by Eckberth [4].

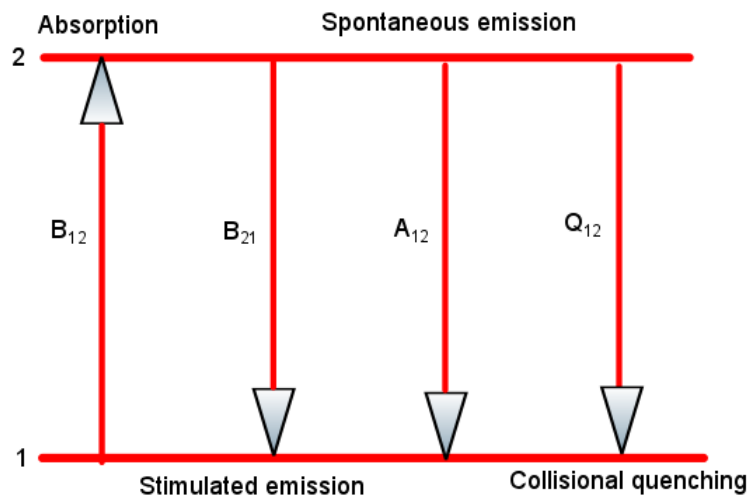


Figure 2.1: 2-level LIF model. 1 representing the ground state while 2 represents the excited state. B_{12} , B_{21} , A_{21} , Q_{21} represent the rate constants for absorption, stimulated emission, spontaneous emission and collisional quenching, respectively.

Figure 2.1 represents a system of two electronic energy levels within an atom/molecule and the different processes that occur in relation to LIF. Absorption is the process of transferring the ground state molecules to the excited state using photons. For stimulated emission photons de-excite the molecules to the ground state with the molecules emitting radiation with the same wavelength, phase and direction as the photons used for the de-excitation. Collisional quenching is radiation-less de-excitation of the excited molecules due to collisions with surrounding molecules.

The decay of the excited molecules through stimulated emission and collisional quenching reduce the amount of excited molecules and thereby the fluorescence produced. Under certain conditions, the excited molecules may also undergo photo-ionization where they are ionized by photons or make a radiation less transition to an unstable excited state, a process referred to as predissociation [4]. These two processes would introduce additional losses to the excited molecules and further reduce the overall amount of fluorescence produced.

2.3.1 Fluorescence signal

The power of the fluorescence signal F , is given by Equation 2.5 [4];

$$F = h\nu l A N_2 A_{21} \frac{\Omega}{4\pi} = h\nu l A \frac{\Omega}{4\pi} N_1^0 \frac{B_{12}}{B_{12} + B_{21}} \frac{A_{21}}{1 + I_{sat}^v / I_v} \quad (2.5)$$

where $h\nu$ is the photon energy, A focal area of the laser beam, l axial length along the beam from which fluorescence is observed, Ω is the solid collection angle, N_2 is the population in the excited state, N_1^0 is the population in the ground state before laser excitation, I_v is the incident laser spectral irradiance and I_{sat}^v is the saturation laser irradiance given by:

$$I_{sat}^v = \frac{(A_{21} + Q_{21})c}{B_{12} + B_{21}} \quad (2.6)$$

The fluorescence signal depends on the laser irradiance I_v and a plot of the fluorescence signal versus the laser irradiance as shown in Figure 2.2 reveals two clear regions; the linear and saturated regime.

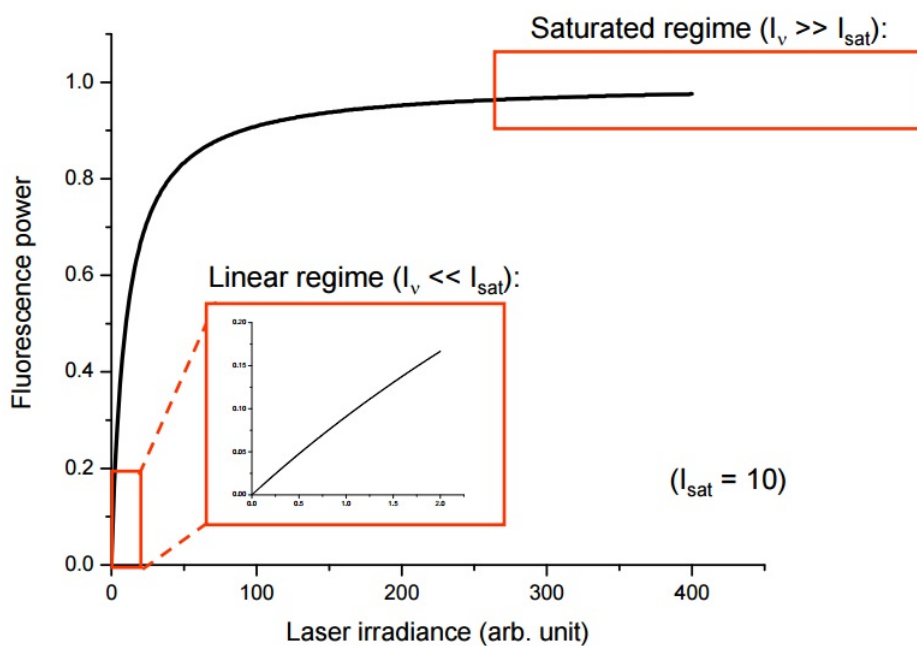


Figure 2.2: Plot showing the dependence of the fluorescence signal on laser irradiance.

In the linear region, the fluorescence signal is proportional to the input laser irradiance; therefore, an increase in the laser irradiance will result in an increase in the signal. The laser irradiance is low in this region such that $I_v \ll I_{sat}$. Therefore equation 2.5 can be simplified to

$$F = hvIA \frac{\Omega}{4\pi} N_1^0 \frac{B_{12}}{B_{12} + B_{21}} \frac{A_{21} I_v}{I_{sat}^v} \quad (2.7)$$

Substituting equation 2.6 into equation 2.7, the power of the fluorescence signal simplifies to:

$$F = \frac{hv}{c} IA \frac{\Omega}{4\pi} N_1^0 B_{12} I_v \frac{A_{21}}{A_{21} + Q_{21}} \quad (2.8)$$

Quantitative fluorescence measurements for determination of N_1^0 in this region are usually very difficult. The quenching rate Q_{21} has to be evaluated and is dependent on the temperature and the flame molecular composition [4]. Therefore, the temperature and quenching species in the flame have to be measured and used together with data on quenching cross sections to make quenching corrections [4]. This requires relevant cross section data and the concentration of the quenching species which is a time consuming exercise to determine. Furthermore, the quenching rate is usually much higher than the rate of spontaneous emission and results in the fluorescence efficiency being less than one which reduces the sensitivity of fluorescence measurements done in this region.

To avoid quenching effects saturated LIF can be performed with excitation in the saturation region as seen in Figure 2.2. The input laser irradiance is then higher than the saturation laser irradiance ($I_v \gg I_{sat}$) resulting in maximum fluorescence signal. Therefore, $1 + I_{sat}/I_v \sim 1$ and Equation 2.5 simplifies to

$$F = hvIA \frac{\Omega}{4\pi} N_1^0 \frac{B_{12}}{B_{12} + B_{21}} A_{21} \quad (2.9)$$

The fluorescence signal from saturated LIF, becomes independent of both the laser irradiance and quenching effects. This results in very high sensitivity of the fluorescent measurements.

Complete saturation is however, difficult to achieve during measurements for various reasons. At certain wavelengths, obtaining high enough laser irradiance necessary for saturation might be difficult. The spatial profile of a focused laser beam is a Gaussian, and the irradiance at the wings of the beam might be too low to achieve saturation. In addition, it is not possible to maintain saturation during the entire duration of the laser pulse [4].

The two-level model is a simplified scheme of the actual fluorescence process. During the absorption process in Figure 2.1, molecules are usually excited from the lowest vibrational level in the ground state to a vibrational level in the excited electronic state. In addition, rotational states that have very small energy difference exist and are easily populated at room temperature. In a flame where the temperatures are normally very high around 2000 K, the population in the ground state is distributed to several rotational levels. Therefore, during the LIF measurements, the excitation of the molecules is done in such a way that the transition excites molecules from one specific rotational level in the ground state to a rotational level in the excited state.

When the transition is such that the rotational quantum number in the ground state is one more than the rotational quantum number in the excited state, the transition is called

P transition. When the rotational quantum number in the ground state is one less than the rotational quantum number in the excited state, the transition is called R transition. While a Q transition is when the rotational quantum number in the ground state is the same as the rotational quantum number in the excited state. These transitions are summarized in the energy level diagram in Figure 2.3.

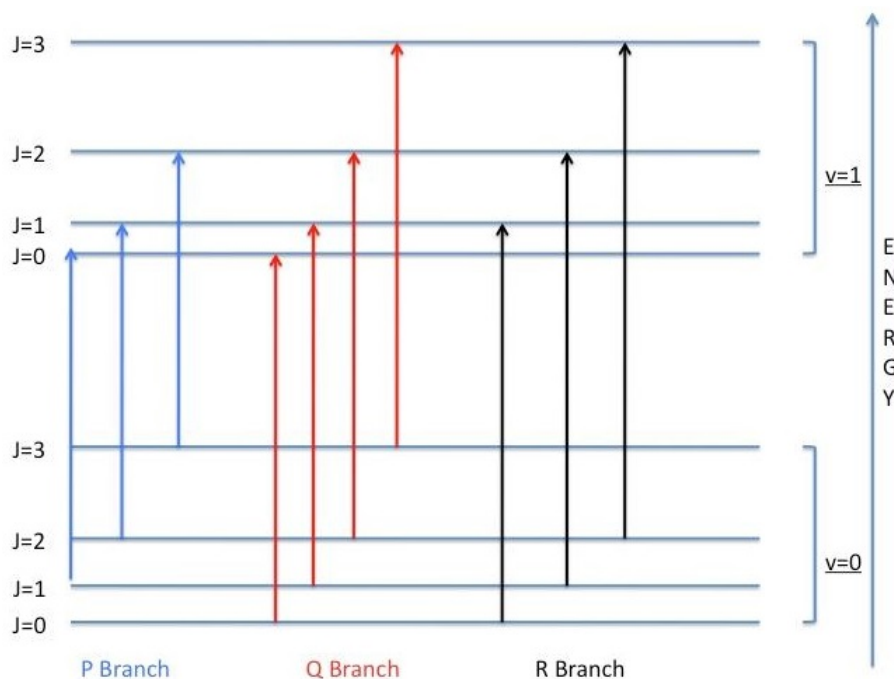


Figure 2.3: Schematic energy level diagram of molecular P, Q and R transitions.

In the excited state, the excited molecules will also be redistributed across several rotational and vibrational levels due to collisions. As a result, they will decay to different vibrational and rotational levels in the ground state producing fluorescence at several wavelengths. The fluorescence is detected from all these different wavelengths to determine the population of the rotational level from which the molecules were initially excited.

In this thesis, laser induced fluorescence measurements of NO molecules was made for rotational transitions in the electronic $A^2\Sigma^+ - X^2\Pi_i$ band employed in previous combustion studies [15].

Chapter 3

Experimental method

3.1 Introduction

The experiments aimed at studying combustion of nitromethane with air/ N_2 mixtures as the oxidizer for both lean and rich stoichiometry. This was done in two parts. The first part involved stabilizing flames lifted off the burner surface. After this had been achieved, temperature profiles and flame chemiluminescence spectra were obtained using a thermocouple and a spectrometer, respectively. The second part involved measurements of NO concentration profiles using saturated LIF.

The flame was stabilized to obtain a flat, premixed laminar flame for which the central part is considered to have temperature and species concentrations varying in only one dimension (vertical) [3]. This gives a very simple geometry that is necessary from a modelling point of view. The chemical simulations are very demanding computationally and a two-dimensional geometry would mean much more complex and time-consuming modelling. The burner plate was metallic, therefore, the flame had to be lifted above the burner surface to prevent scattering of the laser light from the burner surface during measurements.

3.2 Burner setup

The experiments were carried out in premixed laminar flames burning on a heat-flux burner [6] consisting of a porous metal plug. The burner plate is connected to water baths that maintained it at 65 degrees Celsius as seen in Figure 3.1. This reduces heat losses from the burner plate and helps in creating adiabatic conditions. A heating tube connects the fuel-oxidizer mixing panel (consisting of the mass flow controllers and the evaporator) to the burner. The tube is also heated and maintained at 65 degrees Celsius with an insulating cover that prevents heat losses to the surrounding and condensation of nitromethane. A

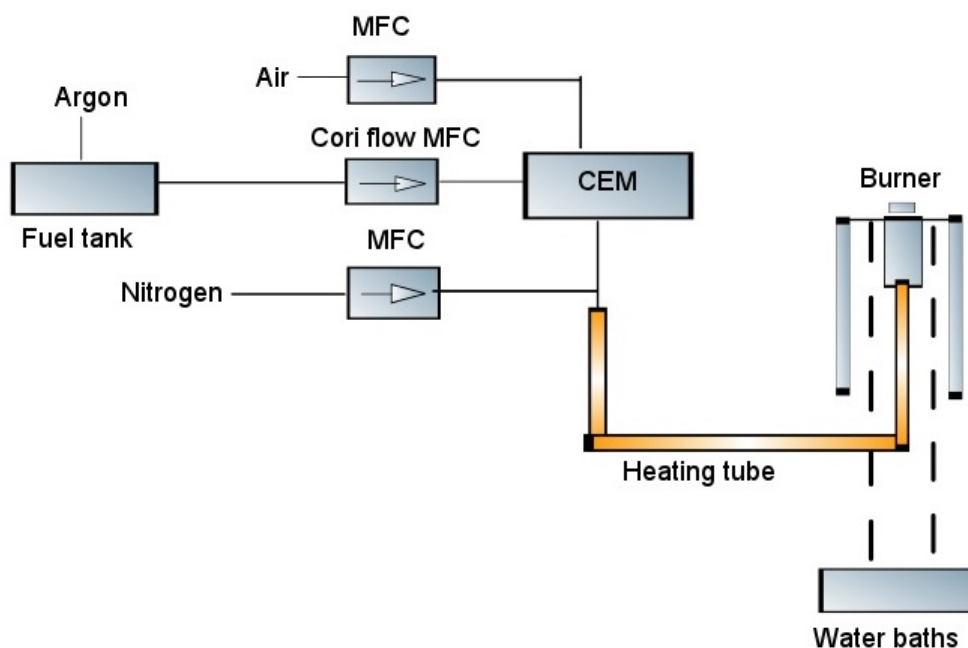


Figure 3.1: A schematic of the burner set-up. MFC stands for mass-flow controllers, CEM controlled evaporator mixer.

steel-plate is placed 2 cm above the burner to stabilize the flame and obtain a stationary flame with minimum oscillations.

Nitromethane is stored in the fuel tank pressurized at 3 bars using argon. The argon is used to generate a liquid flow and prevents it from reacting with air in the reservoir. The fuel flow is controlled using a mass-flow controller for liquid fuels (cori-flow). The controlled evaporator mixer (CEM) has a spiral which is heated to vaporize the liquid nitromethane. Additional mass-flow controllers (MFC) are used to control the flows of the gases to the flame. The flows through the MFC are set and monitored using a LabView computer program.

To stabilize the flame, the burning velocity of the mixture and the flow velocity of the unburnt gas must be matched. The burning velocity is temperature dependent and therefore by varying the flame temperature, the burning velocity is in turn adjusted. This was accomplished by diluting the oxidizer with nitrogen which will reduce the oxygen concentration in the fuel/oxidizer mixture. This decreases the reactions within the flame and therefore lowers the temperature and hence the flame burning velocity, resulting in a raised flame above the burner. The oxidizer composition was varied by adjusting separate flow rates of nitrogen and air. The flame is also stabilized by changing the speed of the unburnt gases. When the velocity of the unburnt gas mixture is higher than the burning velocity of the flame, the reaction zone gets lifted and vice versa. Through changing the velocity of the unburnt gases the burning velocity and unburnt gas velocity were matched. The two flames that were investigated were stabilized using the parameters shown in Table 3.1 .

Equivalence ratio	0.8	1.2
Concentration of Nitrogen in oxidizer	0.18	0.26
Concentration of air in oxidizer	0.82	0.74
Velocity of the gas mixture	20 cm/s	22 cm/s

Table 3.1: Flame stabilization parameters.

3.3 Temperature and flame chemiluminescence measurements

The flame is axially symmetric and therefore the temperature at a certain height is constant and only changes as a function of height above the burner. The temperature of the flame was measured by moving a thin thermocouple vertically along the center of the flame. The heat from the flame generates a voltage in the thermocouple wires that is read out as the temperature of the flame. A type R thermocouple was used which could measure a maximum temperature of 1873 K.

The chemiluminescence radiation emitted from thermally excited flame radical species was measured using a spectrometer (Andor SR-500i-A-R). The chemiluminescence emitted across the horizontal flame reaction and product zones was imaged on the vertical spectrometer slit using a lens of focal length 100 mm placed at distances of 200 mm each from the flame and the spectrometer.

3.4 Laser Induced Fluorescence

The set up for the laser induced fluorescence measurements is shown in Figure 3.2

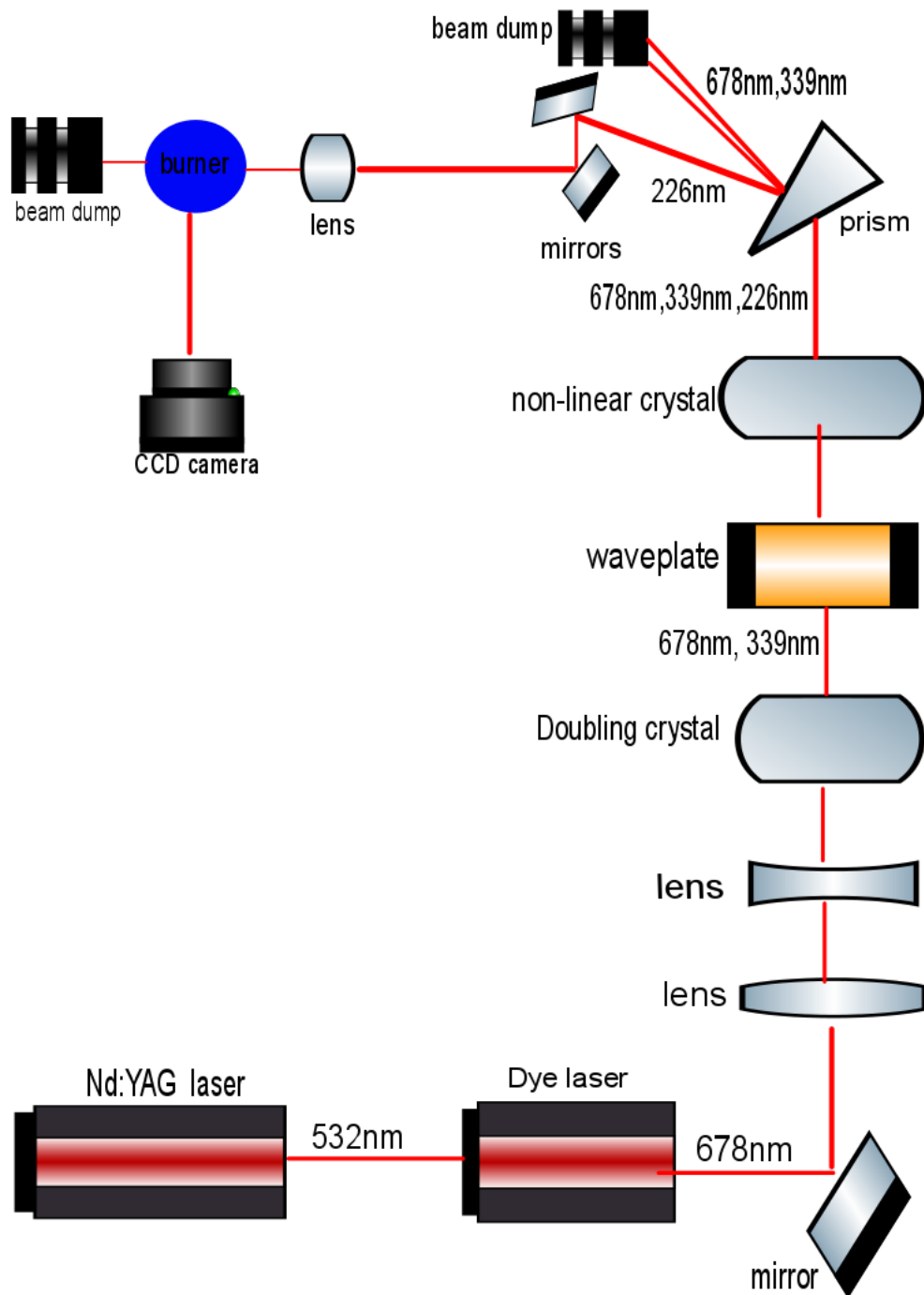


Figure 3.2: The optical set-up for LIF measurements.

Third harmonic generation was used to produce the UV wavelength required for NO excitation since no laser is capable of directly generating it. A Nd:YAG laser (Spectra Physics, PRO 290-10) operated at 532 nm was used to pump a dye laser (Sirah, PRSC-

D-18) using the dye LDS 698 to generate a beam at 673 nm with 140 mJ of energy per pulse. Prior to entering the crystal for doubling the frequency, the size of the 673 nm beam was reduced using a telescope consisting of two lenses of with focal length of 15 mm and -30 mm, respectively. Efficient frequency-doubling requires the so-called phase-matching condition to be fulfilled, which means that the momentum of the photons is conserved, and this is achieved by adjusting the crystal angle.

The fundamental beam and the second harmonic generated have different polarizations which will greatly reduce the efficiency of the third-harmonic-generation process. Therefore, a half-waveplate is used to align their polarizations in the same direction. The two beams are then mixed in the third-harmonic crystal to generate a third beam by means of sum-frequency generation. The crystal mixes the two beams to generate a beam at 224 nm wavelength with 1.2 mJ pulse energy. Similar to the frequency-doubling the sum-frequency/third harmonic generation process requires phase-matching achieved by tuning the crystal angle.

A Pellin Broca prism separates the three beams (678 nm, 339 nm and 226 nm). The 678 nm and 339 nm beams are directed into a beam dump while the 226 nm beam is focused at the center of the burner using a lens of focal length $f=250$ mm to induce saturated fluorescence. Two mirrors positioned before the lens are placed at an angle with one directly above the other. They are used to change the vertical height of the beam across the flame by slightly tilting them. A beam dump behind the burner is used to terminate the beam. The fluorescence signal from the NO is detected using a CCD camera that is placed perpendicular to the direction of the propagating beam. The camera is fitted with a UV lens ($f=105$ mm) to focus the fluorescence emission onto the camera intensifier. A 36 mm extension tube was used to achieve suitable magnification and a long pass filter was used to block out radiation from the laser beam.

The laser beam wavelength was initially scanned between 224 nm to 225 nm and the fluorescence during the scan is monitored, a process referred to as excitation scan measurement. The fluorescence emission peaks obtained from the scan are used to match different vibration-rotational transitions to the laser wavelength. The $Q_2(36.5)$ transition of NO was excited at 224.54 nm and the laser was tuned to perform the saturated LIF measurements at this wavelength. Point wise NO measurements were made at different flame positions by moving the beam vertically along the center of the burner.

Detection using the CCD camera was gated and the recording was triggered from the laser using a small delay ensuring that the camera was open during a 50 ns gate covering the laser pulse and fluorescence event with minimized capturing of continuous background signal from the flame. Furthermore, the fluorescence signal was recorded by averaging 300 exposures for every point measured to average laser pulse-to-pulse variations and hence improves the signal-to-noise ratio of the fluorescence signal detected.

Rayleigh scattering measurements were carried out on nitrogen gas at ambient conditions to calibrate for parameters of the detection system such as the solid angle and detector response. Measurements were made with the nitromethane flow closed and only nitrogen was allowed to flow to the burner. The laser beam was directed at the burner and the scattered signal from the nitrogen was captured by the camera.

3.5 NO concentration evaluation

The concentration of the NO molecules in the flame can be calculated by re-arranging Equation 2.9 to

$$N_1^0 = F \frac{4\pi}{\Omega h\nu l A} \frac{B_{12} + B_{21}}{B_{12}} \frac{1}{A_{21}} \quad (3.1)$$

Equation 3.1 gives the number density concentration of NO molecules in level 1 before laser excitation. However, the high temperatures in the flame will cause distribution of the molecules in the excited state to different rotational levels and the decay of the NO molecules will be distributed across different vibrational levels in the ground state. As a result, the fluorescence radiation will be emitted at multiple different wavelengths. Equation 3.1 is therefore modified to account for these transitions and becomes.

$$N_1^0 = F \frac{4\pi}{\Omega h\nu l A} \frac{B_{12} + B_{21}}{B_{12}} \frac{1}{A_{21}^1 \nu_1 + A_{21}^2 \nu_2 + A_{21}^3 \nu_3 + \dots + A_{21}^n \nu_n} \quad (3.2)$$

The absorption and emission coefficients are obtained from the LIFBASE [17] program. The absorption and emission coefficients B_{12} and B_{21} for the $Q_2(36.5)$ transition line is $9.581 * 10^8 J^{-1} m^3 s^{-2}$. The emission coefficients for the different wavelengths of the NO fluorescence band is given in the table below

Wavelength (nm)	Emission coefficient (s^{-1})
226.502	$9.802 * 10^5$
236.558	$1.448 * 10^6$
247.375	$1.215 * 10^6$
259.040	$7.677 * 10^5$
271.653	$4.080 * 10^5$
285.330	$1.934 * 10^5$

Table 3.2: Table of the NO emission wavelengths and the corresponding emission co-efficients.

The product of the length and the solid angle of the measurement is obtained from the Rayleigh signal. The Rayleigh scattering signal power is given by

$$P_{Ray} = P_i n \left(\frac{\partial \sigma}{\partial \Omega} \right)_{(mix)} \Omega \varepsilon \quad (3.3)$$

P_{Ray} is the Rayleigh power, P_i is the incident laser power, $\left(\frac{\partial \sigma}{\partial \Omega} \right)_{(mix)}$ is the Rayleigh cross section of the mixture, ε is the collection efficiency and n is the concentration. From the ideal gas law, the concentration n at room temperature and atmospheric pressure is obtained as $2.49 * 10^{25} m^{-3}$. The nitrogen Rayleigh cross-section at the laser wavelength is $2.4182 * 10^{-30} m^2$ [16]. The laser power P_i , is the ratio of the pulse energy of 1.2 mJ to the laser pulse duration of 4 ns. The laser therefore delivers peak power of 0.3 MW. The Rayleigh signal detected from scattering by nitrogen molecules was 53,078,219 counts. Since the fluorescence and Rayleigh signals are detected by the same equipment, the collection efficiency is considered to be the same and will cancel out in the calculations. The product of the length and the solid angle of the measurement is 2,932,461 sr.m.

The number density concentration N_1^0 calculated using the Equation 3.2 is the concentration of NO molecules that were on the rotational level $J=36.5$ before laser excitation. However, this is just a fraction of the entire number of NO molecules within the point being measured. Therefore, to determine the entire concentration of the NO molecules at the point of measurement, the concentration of the $J=36.5$ rotational level is divided by the fraction of the NO molecules expected to be within the $J=36.5$ level. This fraction was readily available in the LIFBASE program [17].

Chapter 4

Results and Discussion

4.1 Temperature measurements

The temperature of the flame as a function of the height above the burner is plotted in Figure 4.1 and Figure 4.2 for the fuel lean ($\Phi=0.8$) and fuel rich ($\Phi=1.2$) cases, respectively.

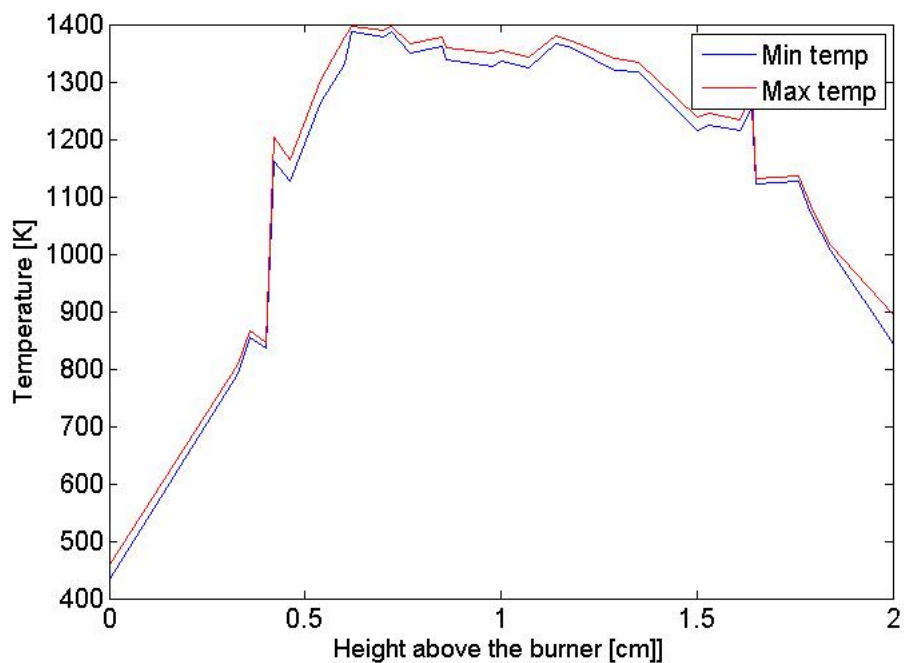


Figure 4.1: Temperature profile at equivalence ratio of 0.8. Min temp and Max temp represent the minimum and maximum temperature recorded at each height, respectively.

The temperature in the vicinity of the burner surface is higher than room temperature. While the water baths maintain the burner surface at temperature 338 K heat is conducted from the reaction zone due to temperature gradients. Figure 4.1, shows that the reaction zone starts around 4 mm above the burner surface due to the steep increase in the temperature. The region below 4 mm represents the pre-heat zone of the flame where the temperature increase is due to the conduction of heat away from the reaction zone.

The rapid temperature rise up to 7 mm results in the highest flame temperature of 1400 K at this position. The combustion of nitromethane can be divided into 3 different zones according to Boyer and Kuo's model [5] as discussed in the theory section. Though not clearly defined in Figure 4.1, the trends in the temperature increase between 4 mm-5 mm, 5 mm-7 mm and 7 mm-12 mm indicates the 3 zones predicted by the model. The flame maintains a rather constant temperature between 7 mm to 12 mm. The steel plate stabilizer located at position 20 mm conducts heat away from the flame resulting in the observed temperature drop to 900 K.

The temperature profile for the fuel rich flame is shown in Figure 4.2.

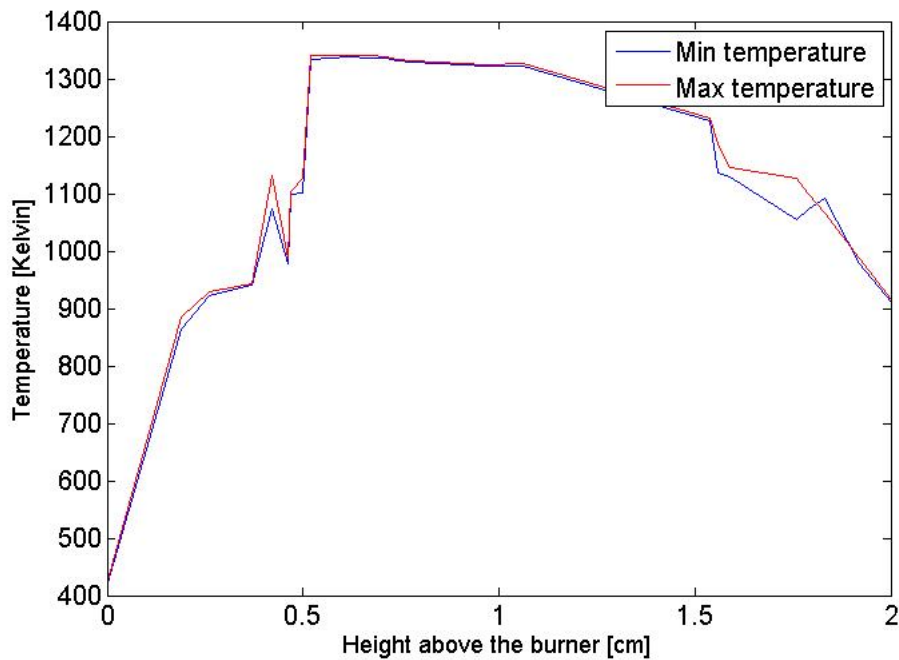


Figure 4.2: Temperature profile at equivalence ratio of 1.2. Min temperature and Max temperature represent the minimum and maximum temperature recorded, respectively.

The temperature profile of the fuel-rich flame also indicates three combustion zones and reaches a maximum temperature of 1350 K in the 3rd zone. However, errors during the measurements account for the flat shape at the beginning of the first zone and the steep temperature drop at the beginning of the second zone. Similar to the lean flame, the temperature drops close to the steel plate stabilizer since it conducts heat away from the flame.

The maximum temperature of the flame was lower for the fuel rich case than the fuel lean case. From the equivalence ratio, it can be seen that the oxygen concentration in the

gas mixture in the rich flames generally has less oxygen concentration than in lean flames. Furthermore, the oxidizer concentration in the rich flames has been more diluted with nitrogen than in the lean flames, therefore some of the nitromethane molecules might not have undergone complete combustion. As a result, the heat released during the combustion of the rich flame is less than in lean flame and hence the lower temperature.

The temperature profiles indicate the three zones that have previously been predicted by various nitromethane combustion models [5]. This has resulted in the nitromethane flame having a stretched reaction zone. However, the temperatures obtained are less than typical flame temperatures and huge temperature differences exist with previous nitromethane temperature profiles measured in nitromethane/oxygen flames [8]. The temperature profile was expected to be slightly lower than those measured by Zhang et al. due to the presence of nitrogen molecules but additional errors due to both the environment and the probing nature of the thermocouple further lowered the temperature. Some points within the reaction zone where the temperature was very high, the thermocouple was glowing due to heating. Under these conditions, loose means that thermocouple temperature does not correspond to the temperature of the flame. The physical probing by the thermocouple also interfered with the flows and concentration gradients within the flame. This led to erroneous results since the structure of the flame had been disturbed. Movement near the flame during the temperature reading also caused some slight turbulence in the flame affecting the accuracy of the measurements.

The temperature profile therefore does not give the exact temperature of the flame, but it does give an estimation of the temperature and the flame behavior as seen from the three zones. More accurate temperature measurements can be achieved by non-intrusive techniques for temperature measurements such as CARS [4].

4.2 Chemiluminescence spectra

The energy from the chemical reactions in flames excites some of the radicals in the flame. Their decay back to the ground state results in the release of radiation, a process called chemiluminescence. The radiation released within the visible region, that is 400-700 nm, is responsible for the color of the flame. A chemiluminescence spectrum of the fuel-lean flame $\Phi=0.8$ is shown in Figure 4.3

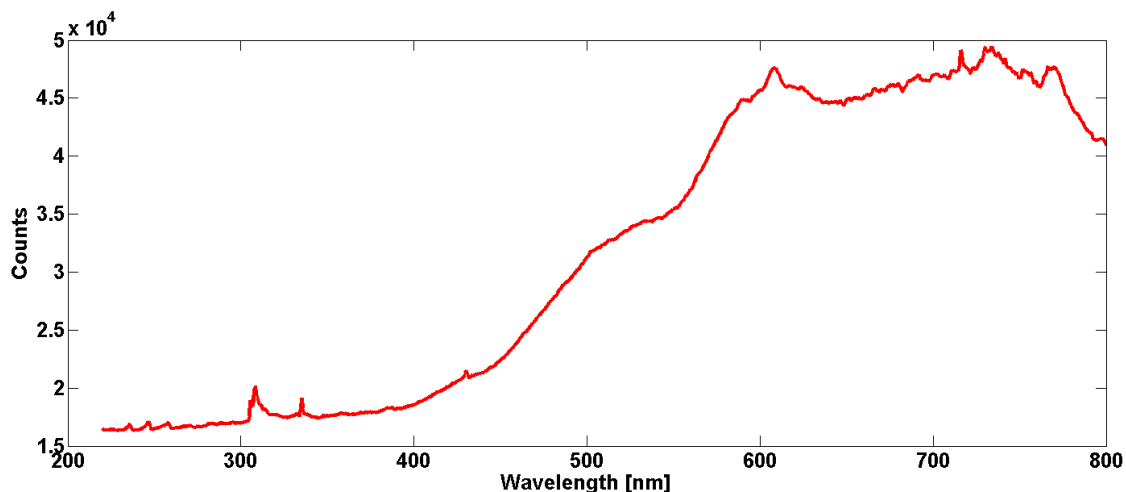


Figure 4.3: The chemiluminescence spectrum of the fuel-lean flame $\Phi=0.8$.

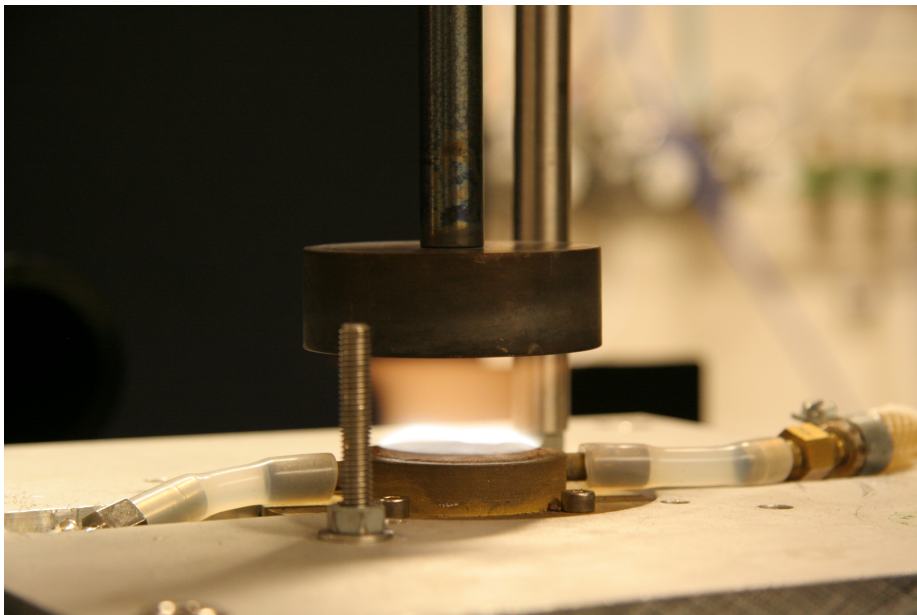


Figure 4.4: Photo of the fuel-lean flame $\Phi=0.8$.

The spectrum of the nitromethane flame shows a very broad and strong emission in the region 460 nm- 800 nm that is attributed to NO_2 [19]. The peaks at the top of the broad

emission are possibly due to the different vibrational bands of NO_2 . The weak peaks at 236 nm, 246 nm and 306 nm represent different NO vibrational bands [17]. The intensity of NO_2 radiation is higher than for the NO radiation suggesting higher concentration of NO_2 than NO in the flame. NO_2 is one of the initial products of nitromethane decomposition and its reduction into NO and N_2 at high temperature produces NO [5]. Furthermore, a small amount of NO is converted to HNO and N_2O reducing the amount of NO. However, since the emission depends on the emission coefficient A_{21} , the higher NO_2 intensity might also be attributed to NO_2 having higher emission coefficient than NO. The spectrum also shows NH peak at 336 nm, a CH peak at 430 nm and OH peaks around 308 nm. The emission from NO_2 is within the visible region and is responsible for the yellow-brown appearance of the nitromethane+air flame as seen in Figure 4.4. The chemiluminescence spectrum and a photo of the fuel-rich $\Phi=1.2$ is shown in Figure 4.5 and Figure 4.6 respectively.

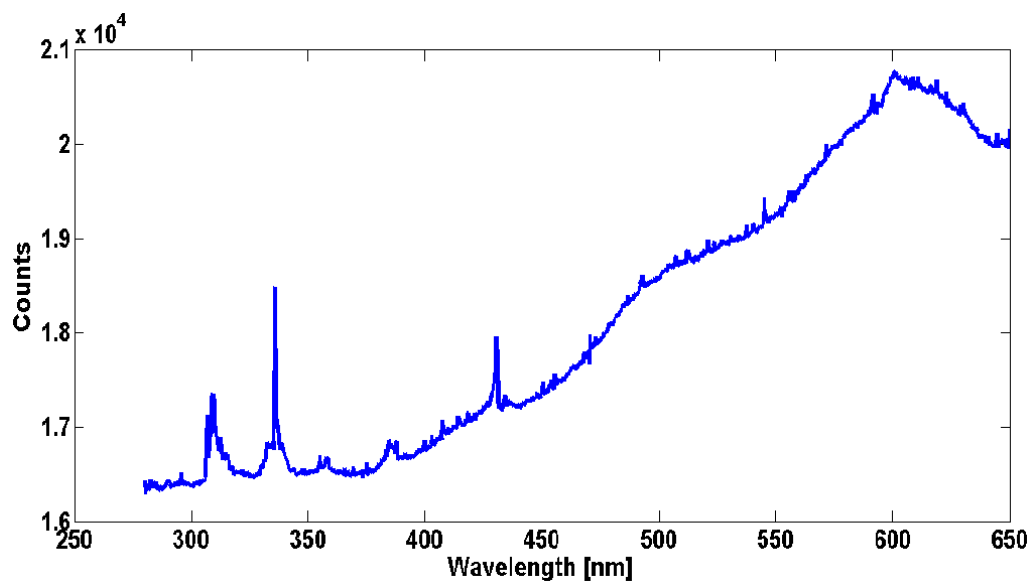


Figure 4.5: The chemiluminescence spectrum at $\Phi=1.2$.

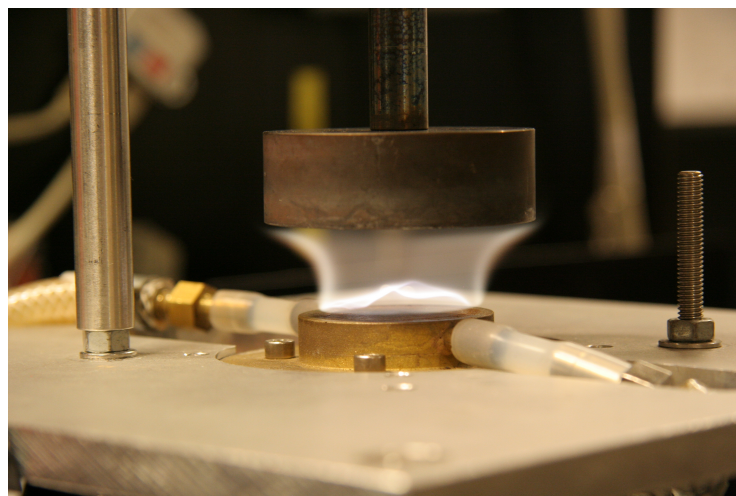


Figure 4.6: Photo of the fuel-rich flame $\Phi=1.2$.

The spectrum for the rich flame has similar peaks to the lean flame since they produce the same radicals. The difference was in the intensity of the radiation at longer wavelengths as seen in Figure 4.7 showing both spectra.

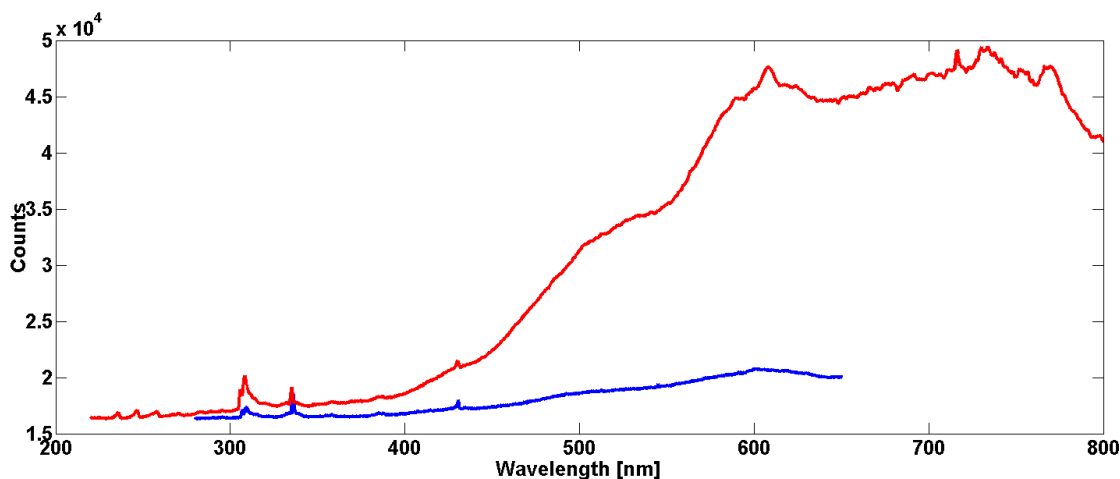


Figure 4.7: Comparison of the emission spectrum at $\Phi = 0.8$ (red) and $\Phi = 1.2$ (blue).

The radiation intensity at wavelengths 460-800 nm was higher from the lean flame than from the rich flame as shown in Figure 4.7. The NO_2 intensity was around three times stronger in the lean case hence the flame appeared more yellow-brown than the rich flame (cf. photos in Figure 4.6 and 4.4). As the intensity is proportional to the concentration of the species, the NO_2 concentration level of the lean flame can be expected to be around 3 times higher than of the fuel-rich flame.

4.3 LIF measurements

4.3.1 Excitation scan

The rotational levels of molecules usually have very small energy differences and a large number of them are populated also at room temperature. The excitation scan performed to excite transitions from different NO rotational levels and measure the fluorescence when the molecules decay is used to assign the different transitions with a specific excitation wavelength. The laser wavelength is then tuned to correspond with the chosen transition. The excitation scan between 224.3-224.7 nm wavelength is shown in Figure 4.8

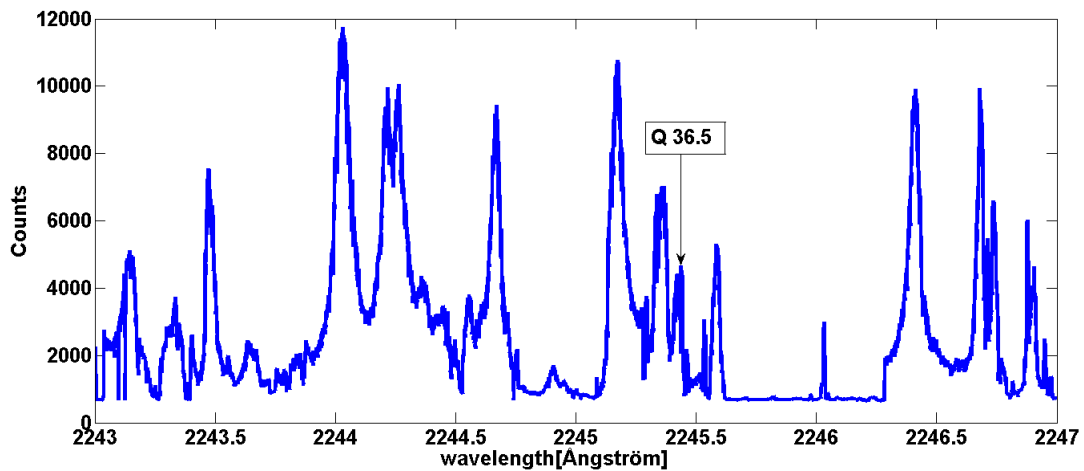


Figure 4.8: Laser excitation scan.

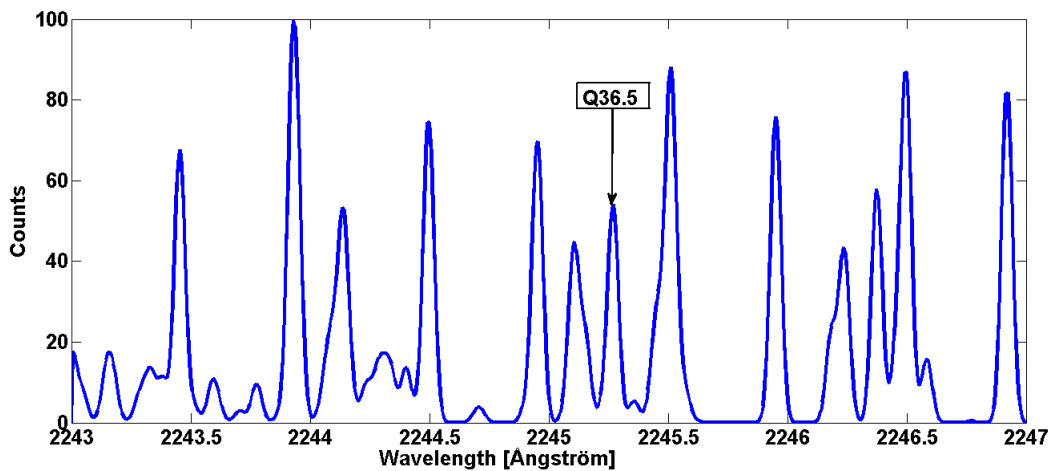


Figure 4.9: Lifbase excitation scan simulation.

Figure 4.8 was compared with the excitation scan simulation from the LIFBASE program [17] in Figure 4.9 to match different NO transitions with the scanned wavelengths. Rotational line $Q_2(36.5)$ that was excited at 224.54 nm was selected for several reasons. The Einstein B coefficient for this transition is greater than that for the $Q_2(26.5)$ transition [17], which has been used in other NO measurements [18]. From Equation 2.6, it can be seen that a higher B constant makes reaching saturation irradiance easier. Furthermore, other species, in particular O_2 having absorption lines in the same spectral region do not interfere spectrally with this NO absorption line [18].

The population of the rotational level was stated to be relatively insensitive to the temperature range of previously investigated flames [18], meaning that the changes in the population of the probed $J=36.5$ level are rather small. This is extremely important to avoid strong temperature dependence on the evaluated NO concentrations. However, when compared to line $Q_2(26.5)$ using the predictions from the LIFBASE program, the population of level $J=36.5$ was observed to be affected more by temperature changes as seen in Figure 4.10.

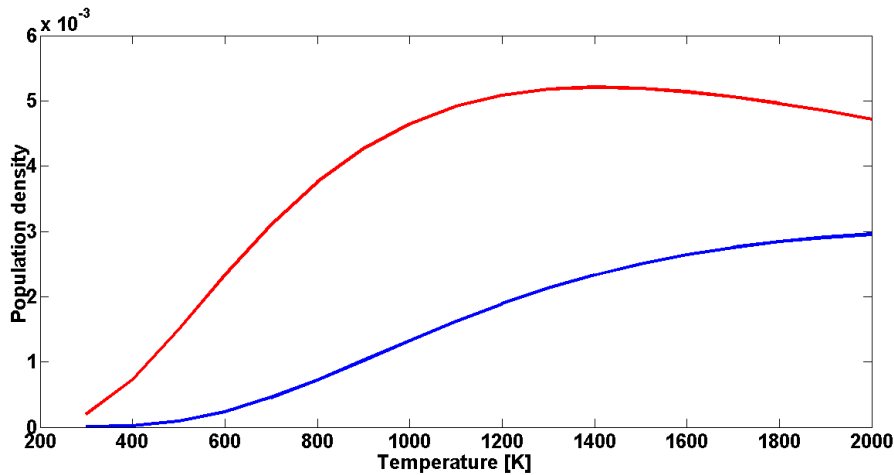


Figure 4.10: NO population dependence on temperature for line $Q_2(36.5)$ (blue line) and line $Q_2(26.5)$ (red line).

The population hardly changes for temperatures above 1000K for the $Q_2(26.5)$ transition line while small changes in the population are observed for the $Q_2(36.5)$ transition line. Since typical flame temperatures are above 1000K, the $Q_2(26.5)$ line would from this aspect have been somewhat better suited for the NO measurements due to its insensitivity in typical flame temperatures.

4.3.2 2-D fluorescence images

Two dimensional fluorescence images for the fuel-rich and fuel-lean flames are shown in Figure 4.11. The laser beam is expanded using a cylindrical lens to induce fluorescence across a large area of the flame and enables monitoring of the changes in the fluorescence signal in the flame both vertically and horizontally.

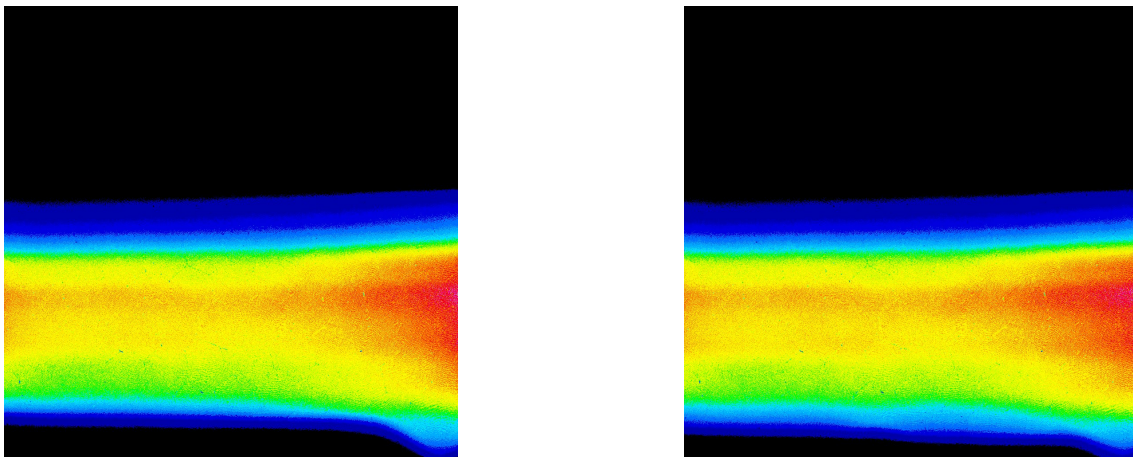


Figure 4.11: 2D fluorescence image at $\Phi= 0.8$ on the left and $\Phi=1.2$ on the right. The image color scale: red =strongest fluorescence, yellow=strong fluorescence, green= average fluorescence, light blue=weak fluorescence, blue=very weak fluorescence, black=no fluorescence.

The laser sheet was created from a laser beam propagating from right to left in the image. The fluorescence intensity is higher on the right and gets weaker towards the left. Since the laser power is spread over a large area when forming the sheet, the fluorescence induced is in the linear regime, where the fluorescence signal is dependent on the laser irradiance. As the beam propagates through the flame, it excites NO molecules and in turn gets attenuated accounting for the drop in the fluorescence intensity across the image.

The region with no fluorescence at the bottom of the images signifies the location of the preheat zone. Immediately above the burner, there is very little fluorescence since the flames are lifted. The fluorescence indicated by the blue and light blue fields, is from NO molecules that have diffused from the reaction zone due to existence of concentration gradient. Furthermore, the lower fluorescence boundary indicates that the flames produced were stable and one dimensional.

The yellow regions on the images represent the product zone of the flames. The region has the highest fluorescence intensity since NO is produced in large quantity in the combustion of nitromethane. The fluorescence intensity drops further above the product zone is attributed to the reduced laser irradiance at the edges of the laser sheet.

4.3.3 NO concentration profiles

The concentration of the NO measured was obtained from the intensity of the fluorescence detected at different vertical positions of the flame. Examples of the fluorescence images obtained during the measurements are shown in Figure 4.12

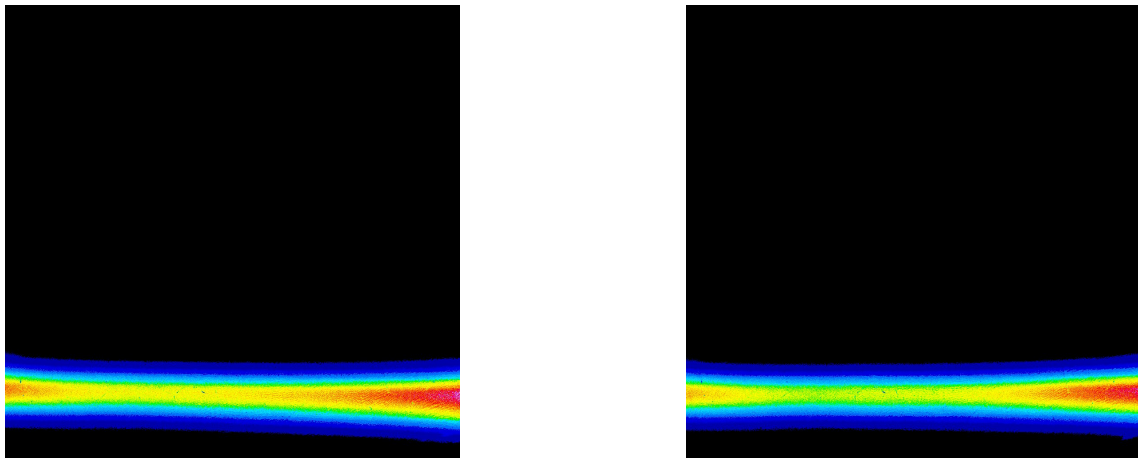


Figure 4.12: Fluorescence images at $\Phi = 0.8$ (left) and $\Phi = 1.2$ (right) respectively.

Figure 4.12 shows the NO fluorescence of the focused beam. The laser beam was focused at the center of the flame which is located in the middle of the image. This is indicated by the converging of the fluorescence signal at the center of the image and diverging towards either side. The laser beam therefore interacted with more NO molecules at the sides of the flame than at the center of the flame. According to Equation 2.9, the fluorescence signal in the saturation region is independent on laser irradiance but dependent on the beam cross sectional area, hence the fluorescence is stronger at the sides than at the center.

The concentration of NO molecules was analyzed at the center where the beam was focused. The laser irradiance along with the spatial resolution (100 micrometers) of the measurements was highest at this point. The spatial resolution was estimated to be 100 micrometers from the rayleigh scattering. The laser spectral irradiance I_v , obtained satisfied the condition for measurements to be done in the saturation region, that is $I_v \gg I_{sat}$. The experimental laser irradiance can be calculated from the pulse energy, the pulse duration and the pulse spectral width ($\Delta\nu$) while the saturation laser irradiance can be calculated using Equation 2.6 using the parameters for the $Q_2(36.5)$ transition and a collisional quenching rate of $10^{-9}s^{-1}$ representative for atmospheric pressure flame conditions [4] as seen below.

$$\frac{P}{A\Delta\nu} \gg \frac{(A_{21} + Q_{21})c}{B_{12} + B_{21}}$$

$$\frac{3 * 10^5}{\pi * (50 * 10^{-6})^2 * 3 * 10^9} \gg \frac{(9.802 * 10^5 + 1 * 10^9) * 3 * 10^8}{2.872 * 10^{17} + 2.872 * 10^{17}}$$

$$12,700 \gg 0.52$$

Thus the measurements were made in the saturation region. The fluorescence intensity from the images is almost equal although the $\Phi = 0.8$ image has slightly higher intensity. This is reflected in the evaluated concentration profiles as seen in Figure 4.13.

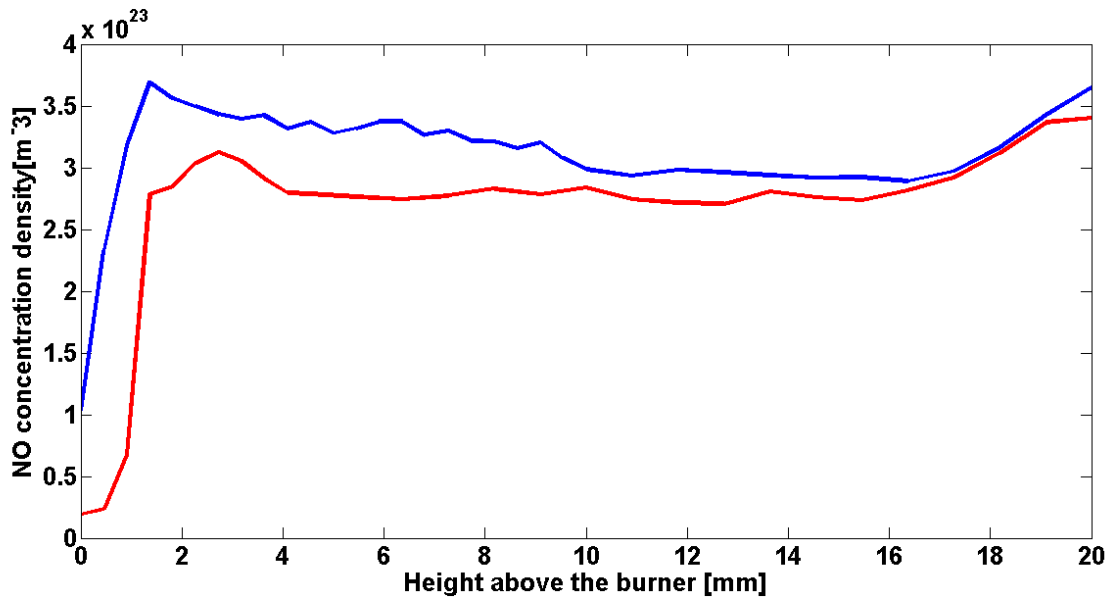


Figure 4.13: NO concentration number density as a function of height for $\Phi = 0.8$ (blue line) and $\Phi = 1.2$ (red line) flame.

The peak NO concentration is at 1.6 mm and 3 mm above the burner for the lean and rich flames, respectively. According to Tian et al. [7], the decomposition of nitromethane to NO_2 and CH_3 occurs mostly in the flame pre-heat zone. The dissociation of NO_2 at high temperatures, accounts for the peak NO concentration. Peak NO concentration occurs in the first zone and therefore signify the beginning of the reaction zone. The concentration drops immediately after the peak can be attributed to the conversion of small amounts of NO to HNO and N_2O which occurs in the first zone. However, the estimated first zone in

Figure 4.13 does not coincide with the first zone estimated from the temperature profiles in Figure 4.1 and Figure 4.3. This is possibly due to the physical probing nature of the thermocouple measurements. The concentration of NO remains relatively constant further above the burner which is in agreement with the prediction of De Jaegere and van Tiggelen [13] that the NO produced in low pressure premixed nitromethane combustion is a non-reactive species.

The increase in the concentration of the NO molecules between 15-20 mm above the height of the burner is inconsistent with nitromethane combustion prediction models. The region coincides with a decrease in the temperature due to its proximity to the steel plate stabilizer, confer Figure 4.1 and Figure 4.3, therefore resulting in an increase in the gas number density. In addition, the population of the $J=36.5$ rotational level corresponding to this region is in turn very low due to its temperature dependence as shown in Figure 4.10. Therefore the population fraction obtained from the LIFBASE [17] program was small resulting in high total NO number density.

The profiles of NO molar fractions, that is, concentrations normalized versus total number density of the gas are shown in Figure 4.14

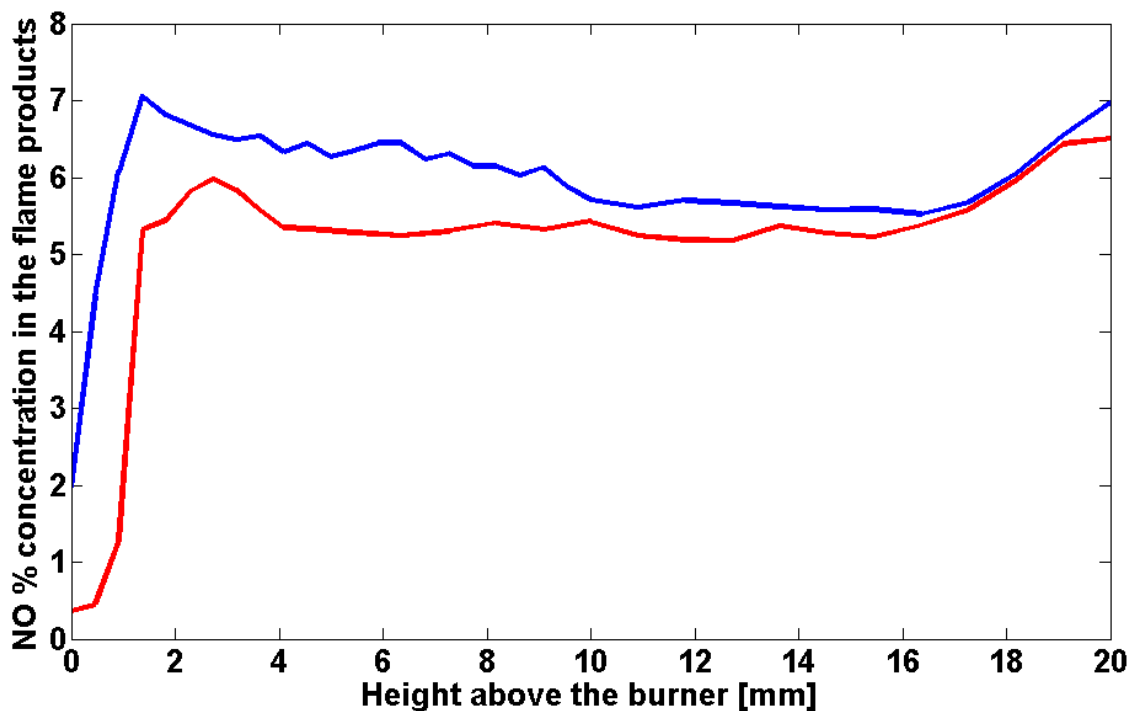


Figure 4.14: NO percentage concentration in the flame products as a function of height for $\Phi=0.8$ (blue line) and $\Phi=1.2$ (red line) flame.

The molar concentration profile also shows a similar trend with the concentration number density profile between 15 mm- 20 mm. However, from the chemistry of nitromethane combustion, no NO production is expected in this region, therefore the shape of the curve is expected to be flat. The temperature obtained at this region is therefore expected to be higher than the temperatures from Figure 4.1 and Figure 4.3. Furthermore, the population fractions acquired from the LIFBASE program and the gas density calculations will be

inaccurate and will account for the unexpected NO increase.

From the evaluated LIF concentrations in Figure 4.14, NO accounted for 6 percent of the total products of nitromethane combustion in the lean flame. The expected NO concentration for the lean flame can be calculated using Equation 2.4. The equation is modified by having nitrogen in the chemical equation since air/nitrogen is used as the oxidizer instead of oxygen, however, the added nitrogen is considered to be an un-reactive species. The experimental flow rates are proportional to the molar concentration of the fuel and the oxidizer gases and used in the equation as shown below:



The NO produced from Equation 4.1 is about 9 percent of the total combustion products. The difference in the measured and the calculated percentage concentration of NO is accounted to several reasons. Firstly, Equation 4.1 considers NO as the only nitrogenous product of nitromethane combustion with the molecular nitrogen constant. However, according to Tian et al. [7] and Zhang et al. [8], molecular nitrogen is produced during the combustion of nitromethane at low pressure. The reactions of HCN, NCO, HNCO, NH and NH₂ radicals with NO either directly or through N₂O leads to formation of nitrogen [8]. Furthermore, N₂O reacts with H atoms to produce nitrogen [8]. Therefore, nitrogen produced could account for the difference. Secondly, the flame produces high concentrations of NO₂ as confirmed from the chemiluminescence spectrum in Figure 4.3 and the orange flame emission visible in the picture 4.4 which is not considered in Equation 4.1. In addition, the thermocouple temperature measurements are lower than typical nitromethane flame temperatures of 1800 K [8]. At 1800 K the flame would have 7.8 percent NO concentration instead of 6.0 percent calculated using the temperature profile. Taking these effects into account, the concentration of NO evaluated from the LIF measurements show good agreement with the expected NO concentration.

Previous studies of rich nitromethane flames have shown high concentrations of HCHO and CH₃OH as products [7]. Along with nitrogen, these products have not been considered in Equation 4.1 and therefore, it is not possible to analyse the rich flame using this chemical equation. Furthermore, the lack of published NO concentration measurements for equivalence ratio of 1.2 makes it difficult to accurately compare the NO concentration measured for the rich flame. However, the rich flame had an NO concentration percentage of 5.5 which showed relatively good agreement with the 8 percent NO concentration results by Tian et al. [7] which was done at pressure of 4.67 kPa and equivalence ratio of 1.39.

Chapter 5

Outlook

Stabilized fuel rich and fuel lean nitromethane flames suitable for both laser diagnostics and modelling were obtained. LIF measurements were successfully carried out in the saturation region. The evaluated concentrations showed good agreement with the estimated chemical reactions and were within the same order of magnitude with kinetic modelling predictions. The NO concentration profiles had similar trends with the modelling predictions apart for the region close to the steel plate stabilizer.

Currently, little research has been conducted on nitromethane combustion using laser-based diagnostics. The non-intrusive nature of these diagnostics will provide more knowledge about the chemical interactions during the combustion process and can be used to validate the prediction models that are currently available. Therefore suggestions for future research projects on nitromethane combustion are suggested below.

Accurate temperature measurements can be done using Coherent anti-Stokes Raman spectroscopy (CARS) to determine the actual temperature profiles of the nitromethane combustion. The non-intrusive nature of the measurements, will eliminate the errors that are normally associated with thermocouples. Furthermore, CARS measurements can also provide the concentration profiles of nitrogen and oxygen within the rich flame. The concentration profile of nitrogen along with that of NO, would help determine whether it is produced due to the interaction of NO or N₂O with other nitrogenous molecules.

The decomposition of nitromethane produces hydrocarbons and nitric oxides which react through numerous interactions. LIF measurements on some of the nitromethane intermediates like NH is therefore recommended to generate further insight into the chemical reactions and the effect on the flame temperature. Furthermore the intermediates may enable validation of Boyer's prediction of multiple reaction zones in nitromethane combustion.

Experimental results by Tian et al. reveal high concentrations of methanol and formaldehyde as products in the combustion of fuel rich nitromethane flames. Therefore, measurements of formaldehyde and methanol are recommended. Formaldehyde can be measured using LIF using the third harmonic of the Nd:YAG laser at 355 nm wavelength. In addition,

Raman spectroscopy of some major flame species, that is, CO, CO₂ along with methanol is suggested to help develop complete understanding of the rich flame.

In addition, LIF measurements to obtain the concentration profile of NO₂ is recommended. The chemiluminescence spectrum obtained in the flame reaction zone revealed that the flames had high concentrations of NO₂ which was responsible for the yellow flame appearance in particular for the lean flame. However, chemical kinetic models and previous experiments predict that NO₂ is only present in the pre-heat zone and the high temperatures in the reaction zone, will cause it to be converted to NO and other nitrogen oxides. The concentration profile would provide further insight about the presence and role of NO₂ in the flame.

The effect of changing the equivalence ratio on the temperature profile and concentration of NO and additional species is suggested. Measurements are to be done at three fuel lean, three fuel rich and at stoichiometry.

Bibliography

- [1] World energy council. *World energy resources survey 2013*
- [2] Mattias Richter. *Chapter 3 of Laser based combustion diagnostics lecture slides*
- [3] S.Svanberg. *Atomic and Molecular Spectroscopy basic aspects and practical applications. Springer, 3rd edition, 2001.*
- [4] A.C .Eckbreth. *Laser diagnostics for combustion temperature and species. Gordon and Breach, 2nd edition,1995.*
- [5] E.Boyer, K.Kuo. *Modeling of nitromethane flame structure and burning behavior, P Combust Inst 31 (2007) 2045–2053.*
- [6] J.D. Naucler, E.J.K. Nilsson, A.A. Konnov *Laminar burning velocity of nitromethane plus air flames: A comparison of flat and spherical flames, Combust Flame 162 (2015) 3803-3809.*
- [7] Zhenyu Tian, Lidong Zhang, Yuyang Li, Tao Yuan, Fei Qi *An experimental and kinetic modeling study of a premixed nitromethane flame at low pressure, P Combust Inst 32 (2009) 311–318.*
- [8] Kuiwen Zhang, Yuyang Li, Tao Yuan, Jianghuai Cai, Pater Glaborg, Fei Qi. *An experimental and kinetic modeling study of a premixed nitromethane flames at low pressure, P Combust Inst 33 (2011) 407-414*
- [9] H.A. Taylor, V.V. Vesselovsk. *The thermal decomposition of nitromethane, J.Phys.Chem, 39 (1934), pp.1095-1101.*
- [10] E.S Starkman *Nitroparaffins as Potential Engine Fuel, Ind.Eng.Chem., 51 (1959), pp.1477-1480.*
- [11] G.J. Germane *A technical review of automotive racing fuels. SAE Technical Paper Series, SAE 852129, 1985.*

- [12] R. Guirguis, D. Hsu, D. Bogan, E. Oran *A mechanism for ignition of high-temperature gaseous nitromethane—The key role of the nitro group in chemical explosives*, *Combust. Flame*, 61 (1985), pp. 51–62
- [13] S. De Jaegere, A. Van Tiggelen *Comparative study of flame propagation in compounds containing nitrogen oxides*, *Combust. Flame*, 3 (1959), pp. 187–200.
- [14] P. Brequigny, G. Dayma, F. Halter, C. Mounaïm-Rousselle, T. Dubois, P. Dagaut *Laminar burning velocities of premixed nitromethane/air flames: An experimental and kinetic modeling study*, *P Combust Inst* 35 (2015) 703-710.
- [15] Katharina Kohse-Höinghaus, Jay B. Jeffries *Applied combustion diagnostics*. Taylor and Francis, 1st edition, 2002.
- [16] R. B. Miles, W. R. Lempert, and J. N. Forkey *Laser Rayleigh scattering*, *Meas Sci Technol* 12, (2001) R33-R51.
- [17] Luque, J. and D.R. Crosley *LIFBASE: Database and spectral simulation (version 1.5)*. SRI International Report MP (1999) 99-009.
- [18] Sameer V. Naik, Normand M. Laurendeau *Laser-saturated and linear LIF measurements of NO in counterflow diffusion flames under non-sooting oxygen-enriched conditions*, *Combust Sci Technol* 174 (2002) 1-21.
- [19] Hall, A. R. and H. G. Wolfhard *Multiple reaction zones in low pressure flames with ethyl and methyl nitrate, methyl nitrite and nitromethane*, *Symposium (International) on Combustion* 6 (1957): 190-199